Long-term real-time chemical characterization of submicron aerosols at Montsec (Southern Pyrenees, 1570 m a.s.l.)

A. Ripoll[1,2]*, M. C. Minguillón[1], J. Pey[3], J. L. Jimenez[4], D. A. Day[4], Y. Sosedova[5], F. Canonaco[5], A. S. H. Prévôt[5], X. Querol[1], and A. Alastuey[1]

[1]Institute of Environmental Assessment and Water Research (IDAEA-CSIC), Jordi Girona 18-26, 08034, Barcelona, Spain

[2] Department of Astronomy and Meteorology, Faculty of Physics, University of Barcelona, Martí i Franquès 1, 08028, Barcelona, Spain

[3]Aix-Marseille Université, CNRS, LCE FRE 3416, Marseille, 13331, France

[4]Department of Chemistry and Biochemistry, and Cooperative Institute for Research in the Environmental Sciences (CIRES), University of Colorado at Boulder, 80309, CO, USA

[5]Paul Scherrer Institute, Laboratory of Atmospheric Chemistry, 5232 Villigen PSI, Switzerland

Correspondence to: A. Ripoll (anna.ripoll@idaea.csic.es)

Abstract. Real-time measurements of inorganic (sulfate, nitrate, ammonium, chloride and black carbon (BC)) and organic submicron aerosols (aerosols with an aerodynamic diameter less than 1 µm) from a continental background site (Montsec, MSC, 1570 m a.s.l.) in the Western Mediterranean Basin (WMB) were conducted for 10 months (July 2011 - April 2012). An Aerosol Chemical Speciation Monitor (ACSM) was co-located with other on-line and off-line PM_1 measurements. Analyses of the hourly, diurnal, and seasonal variations are presented here, for the first time for this region.

Seasonal trends in PM_1 components are attributed to variations in: evolution of the planetary boundary layer (PBL) height, air mass origin, and meteorological conditions. In summer, the higher temperature and solar radiation increases convection, enhancing the growth of the PBL and the transport of anthropogenic pollutants towards high altitude sites. Furthermore, the regional recirculation of air masses over the WMB creates a continuous increase in the background concentrations of PM_1 components and causes the formation of reservoir layers at relatively high altitudes. The combination of all these atmospheric processes results in a high variability of PM_1 components, with poorly defined daily patterns, except for the organic aerosols (OA). OA was mostly composed (up to 90%) of oxygenated organic aerosol (OOA), split in two types: semi-volatile (SV-OOA) and low-volatile (LV-OOA), the rest being hydrocarbon-like OA (HOA). The marked diurnal cycles of OA components regardless of the air mass origin indicates that they are not only associated with anthropogenic and long-range-transported secondary OA (SOA), but also with recently-produced biogenic SOA.

Very different conditions drive the aerosol phenomenology in winter at MSC. The thermal inversions and the lower vertical development of the PBL leave MSC in the free troposphere most of the day, being affected by PBL air masses only after midday, when the mountain breezes transport emissions from the adjacent valleys and plains to the top of the mountain. This results in clear diurnal patterns of both organic and inorganic concentrations. OA was also mainly composed (71%) of OOA, with contributions from HOA (5%) and biomass burning OA (BBOA; 24%). Moreover, in winter sporadic long-range transport from mainland Europe is observed.

The results obtained in the present study highlight the importance of SOA formation processes at a remote site such as MSC, especially in summer. Additional research is needed to characterize the sources and processes of SOA formation at remote sites.

Keywords: high altitude, mountain, remote, continental background, ACSM.

1 Introduction

Earth's climate system is modulated by atmospheric aerosols. Submicron particles (< 1 μm in aerodynamic diameter) play a dominant role in both cloud formation and scattering or absorbing solar radiation (IPCC, 2013). The complexity of aerosol sources and processes results in an uncertainty in the radiative forcing of climate. Aerosol optical properties are connected to direct and indirect climate forcing effects, and they are dependent on particle composition. Moreover, aerosol composition may provide valuable information on aerosol sources and processes. Consequently, long-term measurements of PM_1 chemical composition are needed to better understand aerosol sources, to quantify their lifetime in the atmosphere and to constrain the uncertainties of their climatic influence.

Long-term PM_1 chemical composition measurements are relatively scarce both off-line and on-line. In the last decade, on-line PM_1 chemical composition measurements have been performed using aerosol mass spectrometers (AMS) at a number of locations. Measurements of on-line chemical composition are useful to study hourly variations and daily patterns. Most of these studies, however, correspond to short-term measurement campaigns (typically a month) (e.g. Crippa et al., 2014; Jimenez et al., 2009; Lanz et al., 2010; Ng et al., 2010; Zhang et al., 2007) given the intensive instrument maintenance required and the need of highly-qualified personnel for a good quality dataset.

In contrast to the use of the AMS in relatively short campaigns, the more recently developed Aerodyne Aerosol Chemical Speciation Monitor (ACSM) is becoming a widely used on-line instrument for long-term measurements of PM_1 chemical composition (Budisulistiorini et al., 2014; Canonaco et al., 2013; Petit et al., 2014; Tiitta et al., 2014). The ACSM is built upon the same technology as the AMS, in which an aerodynamic particle focusing lens is combined with high vacuum thermal particle vaporization, electron impact ionization, and mass spectrometry. Modifications in the ACSM design (e.g. lack of particle sizing chamber and components, use of simple and compact RGA mass spectrometer detector), however, allow it to be smaller, lower cost, and simpler to operate than the AMS (Ng et al., 2011c). The ACTRIS (Aerosols, Clouds, and Trace gases Research InfraStructure) European network is evaluating the use of the ACSM as a reliable instrument, which will provide the opportunity to study long-term datasets of PM_1 chemical composition across the continent.

Recent publications have investigated most of the existing worldwide AMS databases (e.g. Crippa et al., 2014; Jimenez et al., 2009; Lanz et al., 2010; Ng et al., 2010; Zhang et al., 2007) and reflected a prevalence of organic aerosols (20 to 90%) in

the submicron fraction, largely independent of the region and type of environment. However, our knowledge on organic aerosol (OA) formation, sources, and atmospheric processing is still very incomplete, especially for secondary organic aerosols (SOA) formed from chemical reactions of gas-phase species (e. g. Donahue et al., 2014; Hallquist et al., 2009; Kroll and Seinfeld, 2008; Robinson et al., 2007; Volkamer et al., 2006). Recent progress has been made in identifying primary organic aerosols (POA) sources (e.g. Elbert et al., 2007; Zhang et al., 2005), but significant gaps still remain in our understanding on the atmospheric evolution of POA after emission (de Gouw and Jimenez, 2009). For these reasons, OA measurements and analysis are required to better understand its chemical evolution in the atmosphere.

The lack of long-term on-line PM_1 chemical composition measurements is especially evident in the Western Mediterranean Basin (WMB), which is characterized by particular atmospheric dynamics strongly influenced by its topography (Jorba et al., 2013; Millan et al., 1997). Over this region, arrival of natural and anthropogenic aerosols as a result of long-range transport from Africa and Europe is frequent (e.g. Pey et al., 2013; Querol et al., 2009; Ripoll et al., 2014; Rodríguez et al., 2001) and accumulation and recirculation processes are frequently observed (Rodriguez et al., 2002). The sources and meteorological controls of PM in the regional background of the WMB have been recently investigated during the DAURE study (Pandolfi et al., 2014a) using an AMS and ^{14}C analyses (Crippa et al., 2014; Minguillón et al., 2011). Furthermore, Ripoll et al. (2015) studied the PM_1 and PM_{10} chemical composition with daily time resolution in the continental and regional background environments in the WMB. In that study, a higher mineral contribution was identified in the continental background due to the preferential transport of African dust at high altitude layers and to the increased regional dust resuspension enhanced by the drier surface and higher convection. Nevertheless, aerosol chemical characterization with higher time resolution is needed to study the origin of specific PM components and the local and/or regional processes, in particular to exploit the information contained in diurnal cycles that is typically not accessible with off-line measurements.

In this study we deployed an ACSM at a high altitude site (Montsec, 1570 m a.s.l.) in the NE of the Iberian Peninsula (42º 03' N, 0º 44' E), representative of the continental background conditions of the Western Mediterranean Basin (WMB) (Ripoll et al., 2014). This environment is under free tropospheric (FT) influence most of the time, although it is exposed to regional pollutants during the summer time and/or under the influence of mountain breezes, and it is affected by trans-boundary incursions of natural and anthropogenic aerosols from Europe and North Africa (Ripoll et al., 2014, 2015). Co-located on-line and off-line PM_1 measurements were also carried out to

complement the ACSM dataset. Hence, the work presented here interprets the real-time variation of inorganic and organic submicron components during 10 months (July 2011 - April 2012), and the types of OA are also studied. Special emphasis is placed on the analysis of diurnal pattern and seasonal variations of chemical components and the main factors influencing these variations.

2 Methodology

2.1 Sampling site

Montsec site (MSC) is located on the highest part of the Montsec d'Ares mountain, at an altitude of 1570 m a.s.l., in a plain near to the edge of a 1000 m cliff to the south, with no wind obstructions present around. It is located in the NE of the Iberian Peninsula (42º03'N, 0º43'E), 50 km S of the Pyrenees and 140 km NW of Barcelona (Fig.S1). A detailed description of this site can be found in Ripoll et al. (2014).

The daily classification of atmospheric episodes affecting MSC was made following the procedure described by Ripoll et al. (2014) using HYSPLIT model from the NOAA Air Resources Laboratory (ARL). Air masses reaching MSC are mainly from the Atlantic (62% of the days) all along the year. From March to October, North African (NAF) episodes are more frequent (17% of the days) and very often are alternated with the summer regional (SREG) scenarios (12% of the days). The winter regional (WREG) scenarios are detected from October to March (11% of the days), as well as the European (EU) episodes (11% of the days). Conversely, the Mediterranean (MED) episodes are detected sporadically (4% of the days).

The boundary layer height was calculated using the Global Data Assimilation System (GDAS) model from the NOAA Air Resources Laboratory (http://www.ready.noaa.gov/READYamet.php) (Fig.S2).

2.2 ACSM sampling and data analysis

The aerosol chemical speciation monitor (ACSM) (Aerodyne Research Inc.) was measuring continuously from July 2011 to April 2012. The ACSM provides real-time mass concentration of submicron particulate organics, nitrate, sulfate, ammonium and chloride via thermal vaporization and electron impact ionization, with detection by a quadrupole mass spectrometer (Ng et al., 2011c). The mass concentration of a given species is determined from the sum of the ion signals at each of its mass spectral fragments and its Ionization Efficiency (IE) (Canagaratna et al., 2007). Since calibration of IEs for all species is not feasible, the Relative Ionization Efficiency (RIE) (compared to that of nitrate) is used (Jimenez et al., 2003). The ammonium nitrate calibration

described by Ng et al. (2011b) was performed using an atomizer (TSI, Constant Output Atomizer Model 3076) for primary aerosol generation, followed by a silica gel diffusion dryer, a differential mobility analyzer (DMA) model TSI 3936, and a condensation particle counter (CPC, TSI 3772). Monodisperse 300 nm ammonium nitrate aerosol particles were used, covering a range of nitrate concentrations from 2 to 15 μg m^{-3}. Several calibrations were conducted throughout the sampling period, and average values of 2.2 x 10^{-11} for nitrate IE and 5.4 for RIE for ammonium were used for the whole dataset. The RIE values used in this study for the rest of the species were those usually applied in AMS ambient concentrations: 1.4 for OA and 1.1, 1.2, and 1.3 for nitrate, sulfate, and chloride, respectively (Canagaratna et al., 2007). RIE for sulfate was experimentally determined one year later and was found to be 1.26, although the default value was used for the current dataset. A time resolution of 62 minutes was used as a result of 12 scans (1 open and 1 filtered) per data point with a scan speed of 1 s amu^{-1}.

The ACSM data were analyzed with the standard ACSM data analysis software version 1.5.3.2 (Aerodyne Research Inc.) written in Igor Pro 6 (WaveMetrics, Inc., Lake Oswego, OR, USA). As the ACSM was measuring continuously for a long time, the standard correction for instrument sensitivity drifts was applied to the dataset based on the inlet pressure and N_2 signal. Finally, mass concentrations were corrected using a Collection Efficiency (CE) to account for the particle bounce of aerosols on the vaporizer. The composition-dependent CE was calculated as described by Middlebrook et al. (2012) and was close to 0.45 for most of the time. Since for most ambient studies a 0.5 CE value is found to be representative with data uncertainties generally within ±20% (Canagaratna et al., 2007), and since our ACSM concentrations using CE=0.5 were in good agreement with concentrations from other co-located instruments, a CE of 0.5 was used.

The organic components were further investigated by applying Multilinear Engine (ME-2) (Paatero, 1999) to the organic mass spectra. With the ME-2, the user can introduce a priori information about sources with the so-called a-value approach. Hence, the user inputs one or more factor profiles and a constraint defined by the a-value, which determines the extent to which the output profile can differ from the profile fed to the model. The source apportionment of OA was performed applying ME-2 using the custom software tool of Source Finder (SoFi) version 4.8 developed by Canonaco et al. (2013). The ME-2 analysis was carried out separately for the summer period (14 Jul 11 – 24 Sep 11) and the winter period (10 Jan 12 – 7 Mar 12). Only *m/z*<=100 were used for source apportionment of OA because: a) the signals of *m/z*>100 account for a minor fraction of the total organic mass (on average, 2 %), b) the *m/z*>100 have larger

uncertainties, and c) the large interference of naphthalene signals (used for *m/z* calibration of the ACSM) at these *m/z* (e.g., m/z 127, 128, and 129) (Sun et al., 2012).

2.3 Co-located measurements used in this study

MSC has been permanently equipped with aerosol monitoring instrumentation since January 2010 and some of these measurements were used in this study. 24-h PM_1 samples were collected every 4 days on 150 mm quartz micro-fiber filters (Pallflex QAT) using high volume samplers (30 m^3 h^{-1}, MCV CAV-A/MSb) equipped with MCV PM_1 cut-off inlets. Daily PM_1 mass concentrations were determined by off-line gravimetric procedures according to the EN 12341 standard (CEN, 1999), i.e. at 20ºC temperature and 50% relative humidity. Furthermore, PM_1 chemical composition was obtained as described by Ripoll et al. (2015) using inductively coupled plasma atomic emission spectroscopy (ICP-AES) and mass spectrometry (ICP-MS) for major and trace elements, respectively, ion high performance liquid chromatography (HPLC) and selective electrode for ions concentrations, and thermal-optical method (using the EUSSAR 2 protocol) for elemental carbon (EC) and organic carbon (OC) concentrations. Real-time PM_1 mass concentrations were continuously measured by an optical particle counter (OPC, Model GRIMM 1.107 calibrated with different latex PSL refraction index 1.59). PM_1 30-minute data were daily averaged and subsequently corrected by comparison with 24-h standard gravimetric mass measurements. The absorption coefficient was measured continuously at 637 nm using a Multi Angle Absorption Photometer (MAAP, model 5012, Thermo). Equivalent black carbon (BC) mass concentrations (Petzold et al., 2013) were calculated by the MAAP instrument software by dividing the measured absorption coefficient σ_{ap} (λ) by 6.6 m^2 g^{-1}, which is the instrument default mass absorption cross section (MAC) at 637 nm (Müller et al., 2011; Petzold and Schönlinner, 2004). Particle scattering (σ_{sp}; 0º-360º) and hemispheric backscattering (σ_{bsp}; 90º-270º) coefficients at three wavelengths (450nm, 525nm, 635nm) were measured with a LED-based integrating nephelometer (model Aurora 3000, ECOTECH Pty, Ltd, Knoxfield, Australia).

Finally, all meteorological data were measured by the Catalonian Meteorological Service from the Montsec d'Ares station. Gaseous pollutants (O_3, NO, NO_2, CO and SO_2) were measured using real-time monitors belonging to the Department of Environment of the Autonomous Government of Catalonia. NO and NO_2 concentrations were measured using a Thermo Scientific instrument, Model 42i-TL; CO using a Teledyne 300 EU Gas filter correlation analyzer; O_3 using a MCV 48AV UV photometry analyzer; and SO_2 using a Teledyne 100 EU UV fluorescence analyzer.

In addition to these routine measurements, 2 intensive campaigns were performed in July - August 2011 and January - February 2012. During these intensive campaigns PM_1 filters were collected daily and a scanning mobility particle sizer (SMPS) was installed to measure particle number size distribution of mobility diameters 11-350 nm in the summer campaign, and 8-450 nm in the winter campaign. The SMPS system comprises a classifier unit (Model TSI 3080) and a differential mobility analyzer (DMA, Model TSI 3081) connected to a condensation particle counter (CPC, Model TSI 3772). The SMPS data for the winter campaign were also used to estimate the mass concentration to compare with the ACSM data. To this end, the volume size distributions were calculated from the measured particle number distributions assuming sphericity. The total volume concentrations were computed by integrating over the measured particle range and converted to mass concentration using the estimated composition-dependent density, calculated using the chemical composition given by the ACSM and the equation of Salcedo et al. (2006). Average concentrations shown in the whole paper are arithmetic~~al~~ averages unless otherwise specified.

3 Results and discussion

3.1 Submicron aerosol mass concentrations

In order to establish the consistency of the different measurements during this study, the sum of the ACSM species (= sulfate + nitrate + ammonium + OA + chloride) and the BC mass concentrations was compared with the co-located PM_1 and light scattering measurements (Fig. 1). The scatter plots of ACSM plus BC concentrations versus PM_1 concentrations from the OPC and SMPS showed strong correlations (R^2=0.72 and R^2=0.87, respectively) and slopes close to unity (slope=0.94 and intercept=0.09 for the ACSM+BC vs. OPC, and slope=1.21 and intercept=0.86 for the ACSM+BC vs. SMPS) (Fig.S3). The differences in the particle size range measured by the different instruments needs to be considered when assessing these comparisons. Moreover, ACSM plus BC concentrations were also highly correlated with light scattering at 525 nm determined by the nephelometer (R^2=0.85, Fig.S3). The high degree of agreement is also apparent in the time series plots of PM_1 shown in Fig. 1.

The average concentration (25^{th}, 50^{th}, 75^{th} percentiles) of the ACSM + BC mass during this study (July 2011 - April 2012) was 4.9 µg m^{-3} (0.9, 2.8, 7.9 µg m^{-3}) (Table S1), which is similar to the 2010-2012 average reported by Ripoll et al. (2014) from OPC measurements (5.0 µg m^{-3}). For the sake of brevity only summer (14 Jul 11 – 24 Sep 11) and winter (10 Jan 12 – 7 Mar 12) hourly variation will be discussed in the following sections, given that hourly variation in spring was similar to summer and that

in fall was similar to winter. The seasonal average PM_1 concentrations were higher in summer (7.5 µg m^{-3} (3.4, 7.1, 10.5 µg m^{-3}), Table S1) than in winter (4.1 µg m^{-3} (0.8, 1.7, 5.6 µg m^{-3}), Table S1). A similar seasonal pattern has been described at other high altitude sites in Europe (e.g. Carbone et al., 2014; Cozic et al., 2008; Freney et al., 2011; Tositti et al., 2013), being associated with differences in the air mass origin from summer to winter, and also to variations in the planetary boundary layer (PBL) height. The seasonal variation at MSC has been described in detail in recent works (Pandolfi et al., 2014b; Ripoll et al., 2014, 2015), and it has been principally attributed to the seasonal variation of the PBL (Fig.S2). In summer, the stable anticyclonic conditions over this continental area enhance convection increasing the development of the PBL and favoring the transport of anthropogenic pollutants towards high altitude sites such as MSC. The situation in winter is notably different, as the lower vertical development of the PBL over this area leaves high altitude sites in the FT, isolating MSC from polluted air masses. The seasonal variation of PM concentrations at MSC has been also connected to mesoscale and synoptic processes. At MSC, southern flows and regional recirculation episodes are more frequent in summer, whereas clean Atlantic advections and northeastern winds from mainland Europe are more common in winter (Fig.S4 and Table S2) (Pandolfi et al., 2014b; Ripoll et al., 2014, 2015). Moreover, the summer maximum has been ascribed to the more vigorous photochemistry in the atmosphere that enhances the formation of secondary inorganic and organic aerosols (Querol et al., 1999).

3.2 Submicron aerosol chemical composition

Concentrations of ACSM species were daily averaged and compared with off-line measurements from 24-h PM_1 samples, and all species showed strong correlations (R^2 between 0.77 and 0.96, Fig.S5). Different slopes (ACSM vs off-line measurements) were found for each of the species: 1.12 for sulfate, 1.31 for ammonium and 1.35 for nitrate. The relatively higher slope for nitrate, with respect to sulfate, could be attributed to a sampling negative artifact due to the volatilization of nitrate on the off-line samples (Schaap et al., 2004). Ammonium is present as a counterion for sulfate and nitrate, and thus its slope is in between those of the two species.

For the OA, the slope could be interpreted as the OM-to-OC ratio, since the off-line measurements determined organic carbon. This slope was found to be 3.39, however values of 2.2 are more common for aged aerosol (e.g. Aiken et al., 2008; Minguillón et al., 2011; Takahama et al., 2011). This disagreement of a factor of 1.54 may be attributed to different reasons. A negative volatilization artifact may occur in the filters, hence resulting in an underestimation of OC. Alternatively it is possible that the

RIE for OA in the ACSM is larger than the value of 1.4 determined for the AMS, a topic currently being investigated by the ACSM manufacturer, which would result in an overestimation of OA. Similar series of intercomparisons with a similar discrepancy for OA has been found for a one-year dataset (June 2012 – July 2013) with the same instrument at Montseny site (Minguillón et al., 2015) and for a recently reported study in Atlanta, US by Budisulistiorini et al. (2014). Assuming that the disagreement was due to the overestimation by the ACSM, the OA concentrations were corrected dividing by the disagreement factor (1.54) to compare the results with co-located measurements (Fig.S3). The resulting slopes were very similar and hence OA concentrations reported in the present paper were not corrected since further research is needed to better estimate the RIE for OA in the ACSM.

The average of PM_1 chemical composition at MSC during this study (July 2011 - April 2012) is given in Fig. 2. On average, OA was the largest PM_1 constituent (50%), followed by sulfate (20%), nitrate (14%), ammonium (12%), BC (4%) and chloride (1%). As was the case of PM_1 concentrations, all chemical components increased in summer and decreased in winter, with the exception of nitrate (Fig. 2 and Table S1). The higher nitrate concentrations in winter than in summer were also observed in other studies in the Mediterranean region (e.g. Pey et al., 2009; Querol et al., 2009; Ripoll et al., 2015) and this variation was attributed to the high volatility of ammonium nitrate at low humidity and high temperature (Zhuang et al., 1999). At MSC, the summer maximum of the rest of PM components has been mainly ascribed to the higher temperature and solar radiation in summer (Table S2), which enhances atmospheric photochemistry, promoting the formation of secondary inorganic and organic aerosols. All these seasonal characteristics are described in detail in Ripoll et al. (2015).

3.2.1 Summer trends

Time series of PM_1 components during summer time (14 Jul – 24 Sep 2011) are shown in Fig. 3. Wind direction and wind speed, temperature, precipitation and concentrations of nitrogen oxides, sulfur dioxide, and ozone are also depicted. The daily classification of atmospheric episodes affecting MSC is also illustrated in different background colors. On average, during summer the lowest concentrations of all PM_1 components and gases were recorded under the Atlantic advection conditions since these air masses are associated with precipitation, decreased temperature and solar radiation, and strong winds, leading to cleaner atmospheric conditions. Conversely, summer regional episodes lasted for 6 to 11 consecutive days and led to sustained increases of the background concentrations of sulfate, OA and BC at MSC. Despite the limited ACSM data availability during North African episodes, relatively high

concentrations of PM_1 components were observed under this type of episodes, especially BC (Fig. 3).

The diurnal cycles of PM_1 components, gaseous pollutants and meteorological variables are shown in Fig. 4. The summer concentrations of PM_1 components and gases showed no clear diurnal patterns, except for ozone and OA. This lack of defined daily patterns is similar to the findings obtained at the high altitude Puy-de-Dôme station in central France (Freney et al., 2011, the only similar study found at a remote site). For a high altitude site as MSC, the lack of diurnal cycles can be explained by a combination of factors. In summer, the recirculation of air masses over the WMB induced by an abrupt orography (Fig.S1) causes the formation of reservoir layers at any time at relatively high altitudes (Millan et al., 1997; Rodríguez et al., 2003). Moreover, long-range transport from North Africa, which can be more intense at high altitude layers (Ripoll et al., 2015), could also blur the daily patterns since the occurrence of this transport does not depend on the time of the day. These factors result in a lack of well-defined daily patterns but in a high variability of diurnal cycles even within the same type of episode, which is reflected in the similar average daily evolutions and the high standard deviations calculated for the average daily patterns when separated by air mass origin (Fig.S6).

The ozone and OA concentrations had a marked diurnal cycle regardless of the air mass origin (Fig. 4 and Fig.S6) in summer. These different daily patterns with respect to the rest of the gases and chemical components points to the fact that ozone and OA variations are strongly influenced by local/regional processes and not just dominated by long-range transport. Minimum ozone concentrations were recorded between 8:00 and 9:00 UTC (Coordinated Universal Time, which is local time - 1:00h and local summer time - 2:00h), whereas maximum concentrations were measured between 16:00 and 17:00 UTC. In contrast, the highest OA concentrations were observed around 12:00 UTC, and the lowest during the night and in the early morning. The ozone variations may influence those of OA, although the complete understanding of the ozone diurnal evolution is outside the scope of this study. The average increase in OA during the day is likely due to the photooxidation of volatile organic compounds (VOCs). Given that MSC is a remote site, in summer VOCs are most likely dominated by local biogenic emissions (BVOCs), as it was found in the Mediterranean forested area of Montseny (Seco et al., 2011). Hence, the midday increase is likely due to recently-produced biogenic SOA, and to a lesser degree, photooxidation of anthropogenic VOCs.

Despite the marked diurnal cycle of OA regardless of air mass origin, the average increase during the day with respect to average concentrations during the

night was higher under summer regional (2.6 µg m^{-3}) and North African (3.0 µg m^{-3}) episodes than during Atlantic advections (1.3 µg m^{-3}) (Fig.S6). This difference could be caused by the higher SOA formation. This is due to the increase in BVOCs emissions and atmospheric photooxidation caused by the higher temperature and solar radiation (Paasonen et al., 2013; Seco et al., 2011) under summer regional and North African episodes. Furthermore, under these episodes higher concentrations of ozone were measured, which also favors the formation of SOA (via direct oxidation and also by leading to higher OH concentrations). The SOA formation registered at MSC is relatively high when compared to other high altitude sites such as Puy-de-Dôme (Freney et al., 2011). This is in agreement with the modeled SOA emissions over Europe, which identified higher SOA concentrations in Mediterranean environments (Bessagnet et al., 2008). This higher SOA formation is probably due to the higher emissions of BVOCs in the Mediterranean forested areas (up to 3 times higher than Boreal forested areas) (Bessagnet et al., 2008; Lang-Yona et al., 2010; Steinbrecher et al., 2009) and the comparable concentrations of tropospheric ozone with other high altitude European sites (Chevalier et al., 2007). On the other hand, the extra formation of SOA under summer regional and North African episodes might also have a contribution from the photooxidation of anthropogenic VOCs, since Atlantic advections are associated with cleaner atmospheric conditions.

3.2.2 Winter trends

Similar to summer, the lowest concentrations of all PM_1 components and gases in winter (10 Jan 12 – 7 Mar 12) were recorded under the Atlantic advections, whereas the highest were measured when MSC was affected by air masses from mainland Europe and sporadically under regional conditions (Fig. 5). Mediterranean air masses were detected very infrequently and therefore conclusions on their characteristics will not be drawn in the present paper. The relative contribution of different components was similar, with OA representing a somewhat smaller fraction than in summer.

In contrast to what was found in summer, in winter concentrations of most PM_1 components and gaseous pollutants showed much clearer diurnal patterns, with a minimum around 7:00 UTC and a maximum between 14:00 and 15:00 UTC (Fig. 4). Similar patterns have been observed at the Puy-de-Dôme station during a winter campaign (Freney et al., 2011). These daily cycles are probably caused by the fact that MSC is located most of the day within the FT in winter, whereas PBL air masses are only injected upwards after midday (Fig.S2). Moreover, thermal inversions are very frequent from 20:00 to 07:00 UTC. These situations prevent the transport of pollutants from the lower populated areas towards higher altitudes, especially at night. During the

morning, the thermal inversions dissipate due to the radiative warming of the ground and mountain upslope winds develop (e.g. Henne et al., 2004). These mountain winds transport anthropogenic emissions from the adjacent valleys and plains to the top of the mountain, with a maximum upslope transport in the afternoon. Moreover, biogenic emissions influence cannot be ruled out as average winter temperatures are high enough for them to occur (Seco et al., 2011; Steinbrecher et al., 2009). Thus, mountain breezes play an important role in determining the diurnal variation of PM_1 components in winter (Fig. 4), especially under regional conditions. A clear example of the PM_1 components diurnal pattern under winter regional episodes was observed from 22 to 25 February 2012 with PM_1 concentrations (and NO_X) increasing several fold during the afternoon (Fig. 5).

The study of the daily cycles as a function of air mass origin (Fig.S7) showed clear diurnal patterns under winter regional episodes, as mentioned above, and less marked daily patterns when MSC is affected by Atlantic advections and long-range transport from mainland Europe. Under Atlantic episodes the concentrations of PM_1 components were very low and the standard deviations with respect to the average pattern were quite high, resulting in unclear diurnal patterns compared to those under winter regional conditions. During European episodes, which can be more intense at high altitude layers (Ripoll et al., 2015; Sicard et al., 2011), background concentrations of PM_1 components were higher and the midday increment was lower compared to those under winter regional conditions, resulting in less marked daily patterns. These less-marked diurnal cycles are probably due to the fact that the increase of PM_1 components occurs during these episodes regardless of the time of the day. A good example of this less-marked diurnal variation during European episodes was observed from 17 to 19 February 2012 (Fig. 5).

3.3 Characterization of OA components

In order to better characterize the profiles of OA components, the ME-2 analysis was performed separately for the summer period (14 Jul – 24 Sep 2011) and the winter period (10 Jan 12 – 7 Mar 12), since OA components are expected to vary throughout the year. The solution of ME-2 analysis selected for each season was based on several tests, with different number of factors and different a-values, taking into account the correlations with external tracers (including nitrate, sulfate, BC and ozone), the daily patterns of each factor, and the residuals. As a result, a solution of 3 factors was selected for each season. In summer, a hydrocarbon-like OA (HOA), a semi-volatile oxygenated OA (SV-OOA) and a low-volatile oxygenated OA (LV-OOA) (Fig.S8) were resolved. The HOA factor was constrained using an average HOA factor from different

datasets (Ng et al., 2011b), with an a-value of 0.1. The SV-OOA was characterized by a high 43-to-44 ratio, and the LV-OOA was defined by having a dominant peak at *m/z* 44. In winter the 3 factors identified were: hydrocarbon-like OA (HOA), biomass burning OA (BBOA) and oxygenated OA (OOA) (Fig.S8). The HOA and the BBOA factors were constrained based on the profiles from different datasets (Ng et al., 2011b), with an a-value of 0.1 in both factors, and including BC as an additional variable to the ME-2 analysis. The OOA was characterized by a 43-to-44 ratio between those found for the LV-OOA and the SV-OOA in summer, and by having a dominant peak at *m/z* 44. This high signal of *m/z* 44 in the winter OOA indicates a high degree of oxidation, and therefore a dominant aged character during winter. A solution with 4 factors in winter was investigated in order to split the OOA into SV-OOA and LV-OOA, but the resulting profiles did not represent two different OOA types, and the time series showed that one of the factors was mainly representing noise. The HOA profiles obtained for the summer and winter periods were similar and showed similar deviations from the Ng et al. (2011b) spectrum (Fig. S9), since they were constrained with the same anchor HOA profile.

On average, LV-OOA dominated the OA fraction in summer contributing 64%, followed by SV-OOA (26%) and HOA (10%) (Fig. 6), whereas in winter OOA accounted for 71%, BBOA contributed 24%, and HOA contribution decreased to 5% (Fig. 7). The high contribution of OOA components confirms the initial hypothesis of MSC organic components being mostly secondary in their origin, and it is in agreement with what was found in other remote sites (Freney et al., 2011; Raatikainen et al., 2010). Furthermore, the origin of OA has been recently investigated in the Mediterranean forested area of Montseny, and it has been found that SOA accounted for 91% (Minguillón et al., 2011). The low contribution of primary organic components at MSC is in agreement with the location, since the primary organic emissions are mixed and oxidized during their transport from industrial and urban areas to the remote site of MSC.

The diurnal cycles of OA components were studied as a function of air mass origin (Fig. 6 and Fig. 7). A clear daily pattern of OA components was found regardless of the air mass origin, except for Atlantic advections in winter. In summer, the maximum concentrations of LV-OOA and HOA were measured between 12:00 and 13:00 UTC, whereas those of SV-OOA were observed between 11:00 and 12:00 UTC. The LV-OOA has been generally associated with highly oxidized, aged, and long-range-transported aerosol particles (Lanz et al., 2010). Conversely, the SV-OOA has been described as the less oxygenated and semi-volatile fraction of OOA (Ng et al., 2011a) and therefore it has been mostly attributed to SOA formation from more local

emissions (Jimenez et al., 2009). For this reason, the LV-OOA and HOA hourly variations are more influenced by long-range transport than those of SV-OOA, which are strongly influenced by local/regional processes. In winter, the maximum concentrations of the OA components were observed simultaneously around 14:00 UTC. The different daily patterns between seasons can be attributed to the higher production of SOA in summer as opposed to winter, when the maximum daily concentrations are reached later driven by the mountain breezes.

4 Conclusions

This work interprets the real-time variation of inorganic and organic submicron components during 10 months (July 2011 - April 2012) at a high altitude site in southern Europe (Montsec, 1570 m a.s.l.). The aerosol chemical composition was obtained with an ACSM, and co-located on-line and off-line PM_1 measurements were also carried out. The average concentration of the ACSM plus BC mass during this study was 4.9 µg m^{-3}, and on average OA was the foremost PM_1 constituent (50%), followed by sulfate (20%), nitrate (14%), ammonium (12%), BC (4%) and chloride (1%). Discrepancies of OA determined by ACSM with co-located measurements pointed to an overestimation by the ACSM probably caused by the use of the default RIE for OA, which could be lower than the actual one. Further research is needed to better address this issue.

The seasonal variation of PM_1 mass and chemical components concentrations showed similar patterns, with an increase in summer and a decrease in winter, except for nitrate which has high volatility in summer. The seasonal variation was attributed to the evolution of the PBL height throughout the year and to synoptic circulation and meteorological factors. At MSC the higher temperature and solar radiation in summer enhances the convection processes, incrementing the development of the PBL, and augments atmospheric photochemistry, promoting the formation of secondary inorganic and organic aerosols.

The diurnal variation of PM_1 components had no clear diurnal patterns in summer, except for organics. This lack of defined daily patterns was ascribed to the recirculation of air masses that causes the formation of reservoir layers at relatively high altitudes, and to the long-range transport from North Africa. These factors result in a high variability of diurnal cycles even within the same type of episode. Nevertheless, organic concentrations had a marked diurnal cycle regardless of the air mass origin, with maximum concentrations around 12:00 UTC. The OA was dominated by LV-OOA (64%), followed by SV-OOA (26%), and HOA (10%). Hence, the midday increase with

respect to average concentrations during the night was attributed to the formation of SOA.

In winter under regional conditions, concentrations of all PM_1 components showed much clearer diurnal patterns than in summer, with a maximum between 14:00 and 15:00 UTC. These daily cycles were connected to the fact that MSC is located most of the day within the FT, whereas PBL air masses are only injected upwards after midday. However, when MSC was affected by long-range transport from mainland Europe, less marked daily patterns of PM_1 components were observed.

The OA in winter was also mainly secondary (71%), with contributions from BBOA (24%), and HOA (5%). The hourly variation of these factors showed a clear diurnal pattern regardless of the air mass origin, except for Atlantic advections.

To the authors' knowledge, this is one of the first times when real-time submicron aerosol chemical composition is characterized and its variation is interpreted during almost a year in a continental background environment. The results obtained in the present study highlight the importance of the SOA formation processes at such remote site as MSC, which could be the objective of further investigations.

Acknowledgements. This study was supported by the Ministry of Economy and Competitiveness and FEDER funds under the PRISMA (CGL2012-39623-C02-1) and CARIATI (CGL2008-06294/CLI) projects, and by the Generalitat de Catalunya (AGAUR 2009 SGR8 and the DGQA). The research received funding from the European Union Seventh Framework Programme (FP7/ 2007-2013) ACTRIS under grant agreement no 262254. The authors would like to extend their gratitude to the personnel from the COU and the OAdM. We would also like to express our gratitude to the NOAA Air Resources Laboratory (ARL) for the provision of the HYSPLIT transport and dispersion model, and boundary layer height calculation, used in this publication. DAD and JLJ thank DOE (BER/ASR) DE-SC0011105 and NOAA NA13OAR4310063.

References

Aiken, A. C., Decarlo, P. F., Kroll, J. H., Worsnop, D. R., Huffman, J. A., Docherty, K. S., Ulbrich, I. M., Mohr, C., Kimmel, J. R., Sueper, D., Sun, Y., Zhang, Q., Trimborn, A., Northway, M., Ziemann, P. J., Canagaratna, M. R., Onasch, T. B., Alfarra, M. R., Prevot, A. S. H., Dommen, J., Duplissy, J., Metzger, A., Baltensperger, U. and Jimenez, J. L.: O/C and OM/OC ratios of primary, secondary, and ambient organic aerosols with high-resolution time-of-flight aerosol mass spectrometry, Environ. Sci. Technol., 42(12), 4478–4485, doi:10.1021/es703009q, 2008.

Bessagnet, B., Menut, L., Curci, G., Hodzic, A., Guillaume, B., Liousse, C., Moukhtar, S., Pun, B., Seigneur, C. and Schulz, M.: Regional modeling of carbonaceous aerosols over Europe-focus on secondary organic aerosols, J. Atmos. Chem., 61(3), 175–202, doi:10.1007/s10874-009-9129-2, 2008.

Budisulistiorini, S. H., Canagaratna, M. R., Croteau, P. L., Baumann, K., Edgerton, E. S., Kollman, M. S., Ng, N. L., Verma, V., Shaw, S. L., Knipping, E. M., Worsnop, D. R., Jayne, J. T., Weber, R. J. and Surratt, J. D.: Intercomparison of an Aerosol Chemical Speciation Monitor (ACSM) with ambient fine aerosol measurements in downtown Atlanta, Georgia, Atmos. Meas. Tech., 7(7), 1929–1941, doi:10.5194/amt-7-1929-2014, 2014.

Canagaratna, M. R., Onasch, T. B., Wood, E. C., Herndon, S. C., Jayne, J. T., Cross, E. S., Miake-Lye, R. C., Kolb, C. E. and Worsnop, D. R.: Chemical and microphysical characterization of ambient aerosols with the aerodyne aerosol mass spectometer, Wiley Intersci., 26(2), 185–222, doi:10.1002/mas.20115, 2007.

Canonaco, F., Crippa, M., Slowik, J. G., Baltensperger, U. and Prévôt, A. S. H.: SoFi, an IGOR-based interface for the efficient use of the generalized multilinear engine (ME-2) for the source apportionment: ME-2 application to aerosol mass spectrometer data, Atmos. Meas. Tech., 6(12), 3649–3661, doi:10.5194/amt-6-3649-2013, 2013.

Carbone, C., Decesari, S., Paglione, M., Giulianelli, L., Rinaldi, M., Marinoni, A., Cristofanelli, P., Didiodato, A., Bonasoni, P., Fuzzi, S. and Facchini, M. C.: 3-year chemical composition of free tropospheric PM1 at the Mt. Cimone GAW global station – South Europe – 2165 m a.s.l., Atmos. Environ., 87, 218–227, doi:10.1016/j.atmosenv.2014.01.048, 2014.

Carbone, S., Saarikoski, S., Frey, A., Reyes, F., Reyes, P., Castillo, M., Gramsch, E., Jayne, J., Worsnop, D. R. and Hillamo, R.: Chemical Characterization of Submicron Aerosol Particles in Santiago de Chile, Aerosol Air Qual. Res., 13, 462–473, doi:10.4209/aaqr.2012.10.0261, 2013.

CEN: Air quality – Determination of the PM10 fraction of suspended particulate matter. Reference method and field test procedure to demonstrate reference equivalence of measurement methods, EN12341:1999, 1999.

Chevalier, A., Gheusi, F., Delmas, R., Ordóñez, C., Sarrat, C., Zbinden, R., Thouret, V., Athier, G., and Cousin, J.-M.: Influence of altitude on ozone levels and variability in the lower troposphere: a ground-based study for western Europe over the period 2001–2004, Atmos. Chem. Phys., 7, 4311-4326, doi:10.5194/acp-7-4311-2007, 2007.

Cozic, J., Verheggen, B., Weingartner, E., Crosier, J., Bower, K. N., Flynn, M., Coe, H., Henning, S., Steinbacher, M., Henne, S., Collaud Coen, M., Petzold, A. and Baltensperger, U.: Chemical composition of free tropospheric aerosol for PM1 and coarse mode at the high alpine site

602 Jungfraujoch, Atmos. Chem. Phys., 8(2), 407–423, doi:10.5194/acp-8-407-
603 2008, 2008.

604 Crippa, M., Canonaco, F., Lanz, V. A., Äijälä, M., Allan, J. D., Carbone, S.,
605 Capes, G., Dall'Osto, M., Day, D. A., DeCarlo, P. F., Di Marco, C. F., Ehn,
606 M., Eriksson, A., Freney, E., Hildebrandt Ruiz, L., Hillamo, R., Jimenez, J.-
607 L., Junninen, H., Kiendler-Scharr, A., Kortelainen, A.-M., Kulmala, M.,
608 Mensah, A. A., Mohr, C., Nemitz, E., O'Dowd, C., Ovadnevaite, J., Pandis,
609 S. N., Petäjä, T., Poulain, L., Saarikoski, S., Sellegri, K., Swietlicki, E., Tiitta,
610 P., Worsnop, D. R., Baltensperger, U. and Prévôt, A. S. H.: Organic aerosol
611 components derived from 25 AMS datasets across Europe using a newly
612 developed ME-2 based source apportionment strategy, Atmos. Chem.
613 Phys., 14, 6159–6176, doi:10.5194/acp-14-6159-2014, 2014.

614 Donahue, N. M., Robinson, A. L., Trump, E. R., Riipinen, I. and Kroll, J. H.:
615 Volatility and Aging of Atmospheric Organic Aerosol, Top. Curr. Chem., 339,
616 97–144, doi:10.1007/128-2012-355, 2014.

617 Elbert, W., Taylor, P. E., Andreae, M. O. and Pöschl, U.: Contribution of fungi to
618 primary biogenic aerosols in the atmosphere: wet and dry discharged
619 spores, carbohydrates, and inorganic ions, Atmos. Chem. Phys., 7(17),
620 4569–4588, doi:10.5194/acp-7-4569-2007, 2007.

621 Freney, E. J., Sellegri, K., Canonaco, F., Boulon, J., Hervo, M., Weigel, R.,
622 Pichon, J. M., Colomb, A., Prévôt, A. S. H. and Laj, P.: Seasonal variations
623 in aerosol particle composition at the puy-de-Dôme research station in
624 France, Atmos. Chem. Phys., 11(24), 13047–13059, doi:10.5194/acp-11-
625 13047-2011, 2011.

626 De Gouw, J. and Jimenez, J. L.: Organic aerosols in the Earth's atmosphere.,
627 Environ. Sci. Technol., 43(20), 7614–8, doi:10.1021/es9006004, 2009.

628 Hallquist, M., Wenger, J. C., Baltensperger, U., Rudich, Y., Simpson, D.,
629 Claeys, M., Dommen, J., Donahue, N. M., Jenkin, M. E., Jimenez, J. L.,
630 Kiendler-Scharr, A., Maenhaut, W., McFiggans, G., Mentel, T. F., Monod, A.,
631 Prévôt, A. S. H., Seinfeld, J. H., Surratt, J. D., Szmigielski, R. and Wildt, J.:
632 The formation , properties and impact of secondary organic aerosol : current
633 and emerging issues, Atmos. Chem. Phys., 9(14), 5155–5236,
634 doi:10.5194/acp-9-5155-2009, 2009.

635 Henne, S., Furger, M., Nyeki, S., Steinbacher, M., Neininger, B., de Wekker, S.
636 F. J., Dommen, J., Spichtinger, N., Stohl, A. and Prévôt, A. S. H.:
637 Quantification of topographic venting of boundary layer air to the free
638 troposphere, Atmos. Chem. Phys., 4(2), 497–509, doi:10.5194/acp-4-497-
639 2004, 2004.

640 IPCC 2013 in: Climate Change 2013: The Physical Science Basis (Contribution of
641 Working Group I to the Fifth Assessment Report of the Intergovernmental Panel on
642 Climate Change) edited by: Myhre, G., Shindell, D., Breon, F.-M., Collins, W.,
643 Fuglestvedt, J., Huang, J., Koch, D., Lamarque, J.-F., Lee, D., Mendoza, B.,

644 Nakajima, T., Robock, A., Stephens, G., Takemura, T., and H, Z. Cambridge Univ.
645 Press, UK and New York, USA, 2013.

646 Jimenez, J. L., Canagaratna, M. R., Donahue, N. M., Prevot, A. S. H., Zhang,
647 Q., Kroll, J. H., DeCarlo, P. F., Allan, J. D., Coe, H., Ng, N. L., Aiken, A. C.,
648 Docherty, K. S., Ulbrich, I. M., Grieshop, A. P., Robinson, A. L., Duplissy, J.,
649 Smith, J. D., Wilson, K. R., Lanz, V. A., Hueglin, C., Sun, Y. L., Tian, J.,
650 Laaksonen, A., Raatikainen, T., Rautiainen, J., Vaattovaara, P., Ehn, M.,
651 Kulmala, M., Tomlinson, J. M., Collins, D. R., Cubison, M. J., Dunlea, E. J.,
652 Huffman, J. A., Onasch, T. B., Alfarra, M. R., Williams, P. I., Bower, K.,
653 Kondo, Y., Schneider, J., Drewnick, F., Borrmann, S., Weimer, S.,
654 Demerjian, K., Salcedo, D., Cottrell, L., Griffin, R., Takami, A., Miyoshi, T.,
655 Hatakeyama, S., Shimono, A., Sun, J. Y., Zhang, Y. M., Dzepina, K.,
656 Kimmel, J. R., Sueper, D., Jayne, J. T., Herndon, S. C., Trimborn, A. M.,
657 Williams, L. R., Wood, E. C., Middlebrook, A. M., Kolb, C. E., Baltensperger,
658 U. and Worsnop, D. R.: Evolution of organic aerosols in the atmosphere.,
659 Science, 326(5959), 1525–1529, doi:10.1126/science.1180353, 2009.

660 Jimenez, J. L., Jayne, J. T., Shi, Q., Kolb, C. E., Worsnop, D. R., Yourshaw, I.,
661 Seinfeld, J. H., Flagan, R. C., Zhang, X., Smith, K. A., Morris, J. W. and
662 Davidovits, P.: Ambient aerosol sampling using the Aerodyne Aerosol Mass
663 Spectrometer, J. Geophys. Res., 108(D7), 8425,
664 doi:10.1029/2001JD001213, 2003.

665 Jorba, O., Pandolfi, M., Spada, M., Baldasano, J. M., Pey, J., Alastuey, A.,
666 Arnold, D., Sicard, M., Artiñano, B., Revuelta, M. A. and Querol, X.:
667 Overview of the meteorology and transport patterns during the DAURE field
668 campaign and their impact to PM observations, Atmos. Environ., 77, 607–
669 620, doi:10.1016/j.atmosenv.2013.05.040, 2013.

670 Kroll, J. H. and Seinfeld, J. H.: Chemistry of secondary organic aerosol:
671 Formation and evolution of low-volatility organics in the atmosphere, Atmos.
672 Environ., 42(16), 3593–3624, doi:10.1016/j.atmosenv.2008.01.003, 2008.

673 Lang-Yona, N., Rudich, Y., Mentel, T. F., Bohne, A., Buchholz, A., Kiendler-
674 Scharr, A., Kleist, E., Spindler, C., Tillmann, R. and Wildt, J.: The chemical
675 and microphysical properties of secondary organic aerosols from Holm Oak
676 emissions, Atmos. Chem. Phys., 10(15), 7253–7265, doi:10.5194/acp-10-
677 7253-2010, 2010.

678 Lanz, V. A., Prévôt, A. S. H., Alfarra, M. R., Weimer, S., Mohr, C., DeCarlo, P.
679 F., Gianini, M. F. D., Hueglin, C., Schneider, J., Favez, O., D'Anna, B.,
680 George, C. and Baltensperger, U.: Characterization of aerosol chemical
681 composition with aerosol mass spectrometry in Central Europe: an overview,
682 Atmos. Chem. Phys., 10(21), 10453–10471, doi:10.5194/acp-10-10453-
683 2010, 2010.

684 Middlebrook, A. M., Bahreini, R., Jimenez, J. L. and Canagaratna, M. R.:
685 Evaluation of Composition-Dependent Collection Efficiencies for the

686 Aerodyne Aerosol Mass Spectrometer using Field Data, Aerosol Sci.
687 Technol., 46(3), 258–271, doi:10.1080/02786826.2011.620041, 2012.

688 Millan, M. M., Salvador, R., Mantilla, E. and Kallos, G.: Photooxidant dynamics
689 in the Mediterranean basin in summer: Results from European research
690 projects, J. Geophys. Res., 102, 8811–8823, 1997.

691 Minguillón, M. C., Perron, N., Querol, X., Szidat, S., Fahrni, S. M., Alastuey, A.,
692 Jimenez, J. L., Mohr, C., Ortega, A. M., Day, D. A., Lanz, V. A., Wacker, L.,
693 Reche, C., Cusack, M., Amato, F., Kiss, G., Hoffer, A., Decesari, S., Moretti,
694 F., Hillamo, R., Teinilä, K., Seco, R., Peñuelas, J., Metzger, A., Schallhart,
695 S., Müller, M., Hansel, A., Burkhart, J. F., Baltensperger, U. and Prévôt, A.
696 S. H.: Fossil versus contemporary sources of fine elemental and organic
697 carbonaceous particulate matter during the DAURE campaign in Northeast
698 Spain, Atmos. Chem. Phys., 11(8), 23573–23618, doi:10.5194/acp-11-
699 12067-2011, 2011.

700 Minguillón, M. C., Ripoll, A., Pérez, N., Prévôt, A. S. H., Canonaco, F., Querol,
701 X. and Alastuey, A.: Chemical characterization of submicron regional
702 background aerosols in the Western Mediterranean using an Aerosol
703 Chemical Speciation Monitor, Atmos. Chem. Phys. Discuss., 15, 965–1000,
704 doi:10.5194/acpd-15-965-2015, 2015.

705 Müller, T., Henzing, J. S., de Leeuw, G., Wiedensohler, A., Alastuey, A.,
706 Angelov, H., Bizjak, M., Collaud Coen, M., Engström, J. E., Gruening, C.,
707 Hillamo, R., Hoffer, A., Imre, K., Ivanow, P., Jennings, G., Sun, J. Y.,
708 Kalivitis, N., Karlsson, H., Komppula, M., Laj, P., Li, S.-M., Lunder, C.,
709 Marinoni, A., Martins dos Santos, S., Moerman, M., Nowak, A., Ogren, J. A.,
710 Petzold, A., Pichon, J. M., Rodriquez, S., Sharma, S., Sheridan, P. J.,
711 Teinilä, K., Tuch, T., Viana, M., Virkkula, A., Weingartner, E., Wilhelm, R.
712 and Wang, Y. Q.: Characterization and intercomparison of aerosol
713 absorption photometers: result of two intercomparison workshops, Atmos.
714 Meas. Tech., 4(2), 245–268, doi:10.5194/amt-4-245-2011, 2011.

715 Ng, N. L., Canagaratna, M. R., Jimenez, J. L., Chhabra, P. S., Seinfeld, J. H.
716 and Worsnop, D. R.: Changes in organic aerosol composition with aging
717 inferred from aerosol mass spectra, Atmos. Chem. Phys., 11(13), 6465–
718 6474, doi:10.5194/acp-11-6465-2011, 2011a.

719 Ng, N. L., Canagaratna, M. R., Jimenez, J. L., Zhang, Q., Ulbrich, I. M. and
720 Worsnop, D. R.: Real-Time Methods for Estimating Organic Component
721 Mass Concentrations from Aerosol Mass Spectrometer Data, Environ. Sci.
722 Technol., 45(3), 910–916, doi:10.1021/es102951k, 2011b.

723 Ng, N. L., Canagaratna, M. R., Zhang, Q., Jimenez, J. L., Tian, J., Ulbrich, I. M.,
724 Kroll, J. H., Docherty, K. S., Chhabra, P. S., Bahreini, R., Murphy, S. M.,
725 Seinfeld, J. H., Hildebrandt, L., Donahue, N. M., DeCarlo, P. F., Lanz, V. A.,
726 Prévôt, A. S. H., Dinar, E., Rudich, Y. and Worsnop, D. R.: Organic aerosol
727 components observed in Northern Hemispheric datasets from Aerosol Mass

728 Spectrometry, Atmos. Chem. Phys., 10(10), 4625–4641, doi:10.5194/acp-
729 10-4625-2010, 2010.

730 Ng, N. L., Herndon, S. C., Trimborn, A., Canagaratna, M. R., Croteau, P. L.,
731 Onasch, T. B., Sueper, D., Worsnop, D. R., Zhang, Q., Sun, Y. L. and
732 Jayne, J. T.: An Aerosol Chemical Speciation Monitor (ACSM) for routine
733 monitoring of the composition and mass concentrations of ambient aerosol,
734 Aerosol Sci. Technol., 45, 780–794, doi:10.1080/02786826.2011.560211,
735 2011c.

736 Paasonen, P., Asmi, A., Petäjä, T., Kajos, M. K., Äijälä, M., Junninen, H., Holst,
737 T., Abbatt, J. P. D., Arneth, A., Birmili, W., van der Gon, H. D., Hamed, A.,
738 Hoffer, A., Laakso, L., Laaksonen, A., Richard Leaitch, W., Plass-Dülmer,
739 C., Pryor, S. C., Räisänen, P., Swietlicki, E., Wiedensohler, A., Worsnop, D.
740 R., Kerminen, V.-M. and Kulmala, M.: Warming-induced increase in aerosol
741 number concentration likely to moderate climate change, Nat. Geosci., 6(6),
742 438–442, doi:10.1038/ngeo1800, 2013.

743 Paatero, P.: The multilinear engine - a table-driven, least squares program for
744 solving multilinear problems, including the n-way parallel factor analysis
745 model, J. Comput. Graph. Stat., 8(4), 854–888, doi:10.2307/1390831, 1999.

746 Pandolfi, M., Querol, X., Alastuey, A., Jimenez, J. L., Jorba, O., Day, D., Ortega,
747 A., Cubison, M. J., Comerón, A., Sicard, M., Mohr, C., Prévôt, A. S. H.,
748 Minguillón, M. C., Pey, J., Baldasano, J. M., Burkhart, J. . F., Seco, R.,
749 Peñuelas, J., van Drooge, B. L., Artiñano, B., Di Marco, C., Nemitz, E.,
750 Schallhart, S., Metzger, A., Hansel, A., Lorente, J., Ng, S., Jayne, J. and
751 Szidat, S.: Effects of sources and meteorology on particulate matter in the
752 Western Mediterranean Basin: An overview of the DAURE campaign, J.
753 Geophys. Res. Atmos., 119, 4978–5010, doi:10.1002/2013JD021079,
754 2014a.

755 Pandolfi, M., Ripoll, A., Querol, X. and Alastuey, A.: Climatology of aerosol
756 optical properties and black carbon mass absorption cross section at a
757 remote high-altitude site in the western Mediterranean Basin, Atmos. Chem.
758 Phys., 14(12), 6443–6460, doi:10.5194/acp-14-6443-2014, 2014b.

759 Petit, J.-E., Favez, O., Sciare, J., Crenn, V., Sarda-Estève, R., Bonnaire, N.,
760 Močnik, G., Dupont, J.-C., Haeffelin, M. and Leoz-Garziandia, E.: Two years
761 of near real-time chemical composition of submicron aerosols in the region
762 of Paris using an Aerosol Chemical Speciation Monitor (ACSm) and a multi-
763 wavelength Aethalometer, Atmos. Chem. Phys. Discuss., 14(17), 24221–
764 24271, doi:10.5194/acpd-14-24221-2014, 2014.

765 Petzold, A. and Schönlinner, M.: Multi-angle absorption photometry—a new
766 method for the measurement of aerosol light absorption and atmospheric
767 black carbon, J. Aerosol Sci., 35(4), 421–441,
768 doi:10.1016/j.jaerosci.2003.09.005, 2004.

769 Petzold, A., Ogren, J. A., Fiebig, M., Laj, P., Li, S.-M., Baltensperger, U.,
770 Holzer-Popp, T., Kinne, S., Pappalardo, G., Sugimoto, N., Wehrli, C.,
771 Wiedensohler, A. and Zhang, X.-Y.: Recommendations for reporting “black
772 carbon” measurements, Atmos. Chem. Phys., 13(16), 8365–8379,
773 doi:10.5194/acp-13-8365-2013, 2013.

774 Pey, J., Pérez, N., Castillo, S., Viana, M., Moreno, T., Pandolfi, M., López-
775 Sebastián, J. M., Alastuey, A. and Querol, X.: Geochemistry of regional
776 background aerosols in the Western Mediterranean, Atmos. Res., 94(3),
777 422–435, doi:10.1016/j.atmosres.2009.07.001, 2009.

778 Pey, J., Querol, X., Alastuey, A., Forastiere, F. and Stafoggia, M.: African dust
779 outbreaks over the Mediterranean Basin during 2001–2011: PM10
780 concentrations, phenomenology and trends, and its relation with synoptic
781 and mesoscale meteorology, Atmos. Chem. Phys., 13(3), 1395–1410,
782 doi:10.5194/acp-13-1395-2013, 2013.

783 Querol, X., Alastuey, A., Lopez-soler, A., Plana, F. and Puicercus, J. A.: Daily
784 evolution of sulphate aerosols in a rural area , northeastern Spain -
785 elucidation of an atmospheric reservoir effect, Environ. Pollut., 105(3), 397–
786 407, doi:10.1016/S0269-7491(99)00037-8, 1999.

787 Querol, X., Alastuey, A., Pey, J., Cusack, M., Pérez, N., Mihalopoulos, N.,
788 Theodosi, C., Gerasopoulos, E., Kubilay, N. and Koçak, M.: Variability in
789 regional background aerosols within the Mediterranean, Atmos. Chem.
790 Phys., 9(14), 4575–4591, doi:10.5194/acp-9-4575-2009, 2009.

791 Raatikainen, T., Vaattovaara, P., Tiitta, P., Miettinen, P., Rautiainen, J., Ehn,
792 M., Kulmala, M., Laaksonen, A. and Worsnop, D. R.: Physicochemical
793 properties and origin of organic groups detected in boreal forest using an
794 aerosol mass spectrometer, Atmos. Chem. Phys., 10(4), 2063–2077,
795 doi:10.5194/acp-10-2063-2010, 2010.

796 Ripoll, A., Minguillón, M. C., Pey, J., Pérez, N., Querol, X. and Alastuey, A.:
797 Joint analysis of continental and regional background environments in the
798 Western Mediterranean: PM1 and PM10 concentrations and composition,
799 Atmos. Chem. Phys., 15, 1129–1145, doi:10.5194/acp-15-1129-2015, 2015.

800 Ripoll, A., Pey, J., Minguillón, M. C., Pérez, N., Pandolfi, M., Querol, X. and
801 Alastuey, A.: Three years of aerosol mass, black carbon and particle number
802 concentrations at Montsec (southern Pyrenees, 1570 m a.s.l.), Atmos.
803 Chem. Phys., 14(8), 4279–4295, doi:10.5194/acp-14-4279-2014, 2014.

804 Robinson, A. L., Donahue, N. M., Shrivastava, M. K., Weitkamp, E. A., Sage, A.
805 M., Grieshop, A. P., Lane, T. E., Pierce, J. R. and Pandis, S. N.: Rethinking
806 organic aerosols: semivolatile emissions and photochemical aging., Science,
807 315(5816), 1259–62, doi:10.1126/science.1133061, 2007.

808 Rodríguez, S., Querol, X., Alastuey, A., Kallos, G. and Kakaliagou, O.: Saharan
809 dust contributions to PM10 and TSP levels in Southern and Eastern Spain,

Atmos. Environ., 35, 2433–2447, doi:10.1016/S1352-2310(00)00496-9, 2001.

Rodriguez, S., Querol, X., Alastuey, A. and Mantilla, E.: Origin of high summer PM10 and TSP concentrations at rural sites in Eastern Spain, Atmos. Environ., 36(19), 3101–3112, doi:10.1016/S1352-2310(02)00256-X, 2002.

Rodríguez, S., Querol, X., Alastuey, A., Viana, M.-M. and Mantilla, E.: Events affecting levels and seasonal evolution of airborne particulate matter concentrations in the Western Mediterranean., Environ. Sci. Technol., 37(2), 216–222, doi:10.1021/es020106p, 2003.

Salcedo, D., Onasch, T. B., Dzepina, K., Canagaratna, M. R., Zhang, Q., Huffman, J. A., DeCarlo, P. F., Jayne, J. T., Mortimer, P., Worsnop, D. R., Kolb, C. E., Johnson, K. S., Zuberi, B., Marr, L. C., Volkamer, R., Molina, L. T., Molina, M. J., Cardenas, B., Bernabé, R. M., Márquez, C., Gaffney, J. S., Marley, N. A., Laskin, A., Shutthanandan, V., Xie, Y., Brune, W., Lesher, R., Shirley, T. and Jimenez, J. L.: Characterization of ambient aerosols in Mexico City during the MCMA-2003 campaign with Aerosol Mass Spectrometry: results from the CENICA Supersite, Atmos. Chem. Phys., 6(4), 925–946, doi:10.5194/acp-6-925-2006, 2006.

Schaap, M., Spindler, G., Schulz, M., Acker, K., Maenhaut, W., Berner, A., Wieprecht, W., Streit, N., Müller, K., Brüggemann, E., Chi, X., Putaud, J.-P., Hitzenberger, R., Puxbaum, H., Baltensperger, U. and ten Brink, H.: Artefacts in the sampling of nitrate studied in the “INTERCOMP” campaigns of EUROTRAC-AEROSOL, Atmos. Environ., 38, 6487–6496, doi:10.1016/j.atmosenv.2004.08.026, 2004.

Seco, R., Peñuelas, J., Filella, I., Llusià, J., Molowny-Horas, R., Schallhart, S., Metzger, A., Müller, M. and Hansel, A.: Contrasting winter and summer VOC mixing ratios at a forest site in the Western Mediterranean Basin: the effect of local biogenic emissions, Atmos. Chem. Phys., 11(24), 13161–13179, doi:10.5194/acp-11-13161-2011, 2011.

Sicard, M., Rocadenbosch, F., Reba, M. N. M., Comerón, A., Tomás, S., García-Vízcaino, D., Batet, O., Barrios, R., Kumar, D. and Baldasano, J. M.: Seasonal variability of aerosol optical properties observed by means of a Raman lidar at an EARLINET site over Northeastern Spain, Atmos. Chem. Phys., 11(1), 175–190, doi:10.5194/acp-11-175-2011, 2011.

Steinbrecher, R., Smiatek, G., Köble, R., Seufert, G., Theloke, J., Hauff, K., Ciccioli, P., Vautard, R. and Curci, G.: Intra- and inter-annual variability of VOC emissions from natural and semi-natural vegetation in Europe and neighbouring countries, Atmos. Environ., 43(7), 1380–1391, doi:10.1016/j.atmosenv.2008.09.072, 2009.

Sun, Y., Wang, Z., Dong, H., Yang, T., Li, J., Pan, X., Chen, P. and Jayne, J. T.: Characterization of summer organic and inorganic aerosols in Beijing, China

851 with an Aerosol Chemical Speciation Monitor, Atmos. Environ., 51, 250–259,
852 doi:10.1016/j.atmosenv.2012.01.013, 2012.

853 Takahama, S., Schwartz, R. E., Russell, L. M., Macdonald, a. M., Sharma, S.
854 and Leaitch, W. R.: Organic functional groups in aerosol particles from
855 burning and non-burning forest emissions at a high-elevation mountain site,
856 Atmos. Chem. Phys., 11(13), 6367–6386, doi:10.5194/acp-11-6367-2011,
857 2011.

858 Tiitta, P., Vakkari, V., Croteau, P., Beukes, J. P., van Zyl, P. G., Josipovic, M.,
859 Venter, A. D., Jaars, K., Pienaar, J. J., Ng, N. L., Canagaratna, M. R., Jayne,
860 J. T., Kerminen, V.-M., Kokkola, H., Kulmala, M., Laaksonen, A., Worsnop,
861 D. R. and Laakso, L.: Chemical composition, main sources and temporal
862 variability of PM1 aerosols in southern African grassland, Atmos. Chem.
863 Phys., 14(4), 1909–1927, doi:10.5194/acp-14-1909-2014, 2014.

864 Tositti, L., Riccio, A., Sandrini, S., Brattich, E., Baldacci, D., Parmeggiani, S.,
865 Cristofanelli, P. and Bonasoni, P.: Short-term climatology of PM10 at a high
866 altitude background station in southern Europe, Atmos. Environ., 65, 142–
867 152, doi:10.1016/j.atmosenv.2012.10.051, 2013.

868 Volkamer, R., Jimenez, J. L., San Martini, F., Dzepina, K., Zhang, Q., Salcedo,
869 D., Molina, L. T., Worsnop, D. R. and Molina, M. J.: Secondary organic
870 aerosol formation from anthropogenic air pollution: Rapid and higher than
871 expected, Geophys. Res. Lett., 33(17), L17811,
872 doi:10.1029/2006GL026899, 2006.

873 Zhang, Q., Jimenez, J. L., Canagaratna, M. R., Allan, J. D., Coe, H., Ulbrich, I.,
874 Alfarra, M. R., Takami, A., Middlebrook, a. M., Sun, Y. L., Dzepina, K.,
875 Dunlea, E., Docherty, K., DeCarlo, P. F., Salcedo, D., Onasch, T., Jayne, J.
876 T., Miyoshi, T., Shimono, A., Hatakeyama, S., Takegawa, N., Kondo, Y.,
877 Schneider, J., Drewnick, F., Borrmann, S., Weimer, S., Demerjian, K.,
878 Williams, P., Bower, K., Bahreini, R., Cottrell, L., Griffin, R. J., Rautiainen, J.,
879 Sun, J. Y., Zhang, Y. M. and Worsnop, D. R.: Ubiquity and dominance of
880 oxygenated species in organic aerosols in anthropogenically-influenced
881 Northern Hemisphere midlatitudes, Geophys. Res. Lett., 34(13), L13801,
882 doi:10.1029/2007GL029979, 2007.

883 Zhang, Q., Worsnop, D. R., Canagaratna, M. R. and Jimenez, J.-L.:
884 Hydrocarbon-like and oxygenated organic aerosols in Pittsburgh: insights
885 into sources and processes of organic aerosols, Atmos. Chem. Phys.
886 Discuss., 5(5), 8421–8471, doi:10.5194/acpd-5-8421-2005, 2005.

887 Zhuang, H., Chan, C. K., Fang, M. and Wexler, A. S.: Size distributions of
888 particulate sulfate , nitrate , and ammonium at a coastal site in Hong Kong,
889 Atmos. Environ., 33(6), 843–853, doi:10.1016/S1352-2310(98)00305-7,
890 1999.

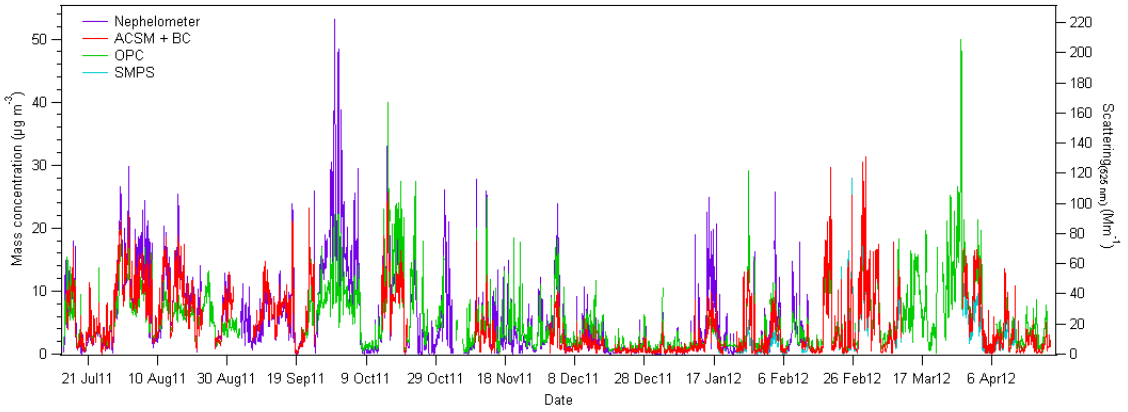

Fig. 1 Time series of PM_1 total mass from co-located measurements and light scattering at 525 nm.

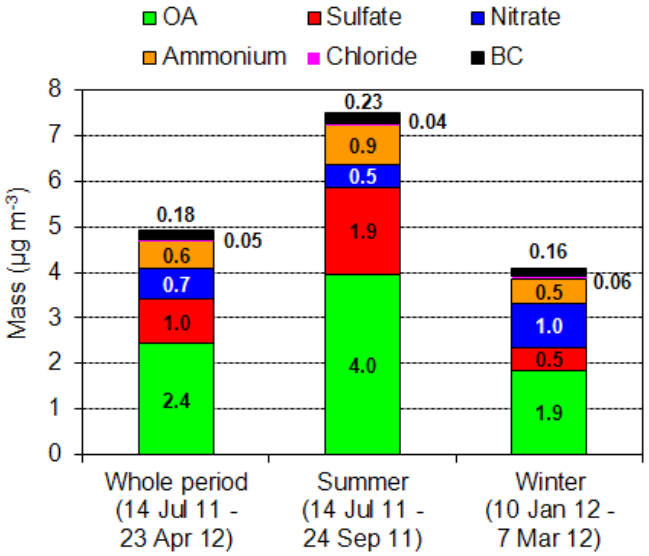

Fig. 2 Average concentrations of PM_1 chemical species measured at Montsec during the whole study, in summer and in winter.

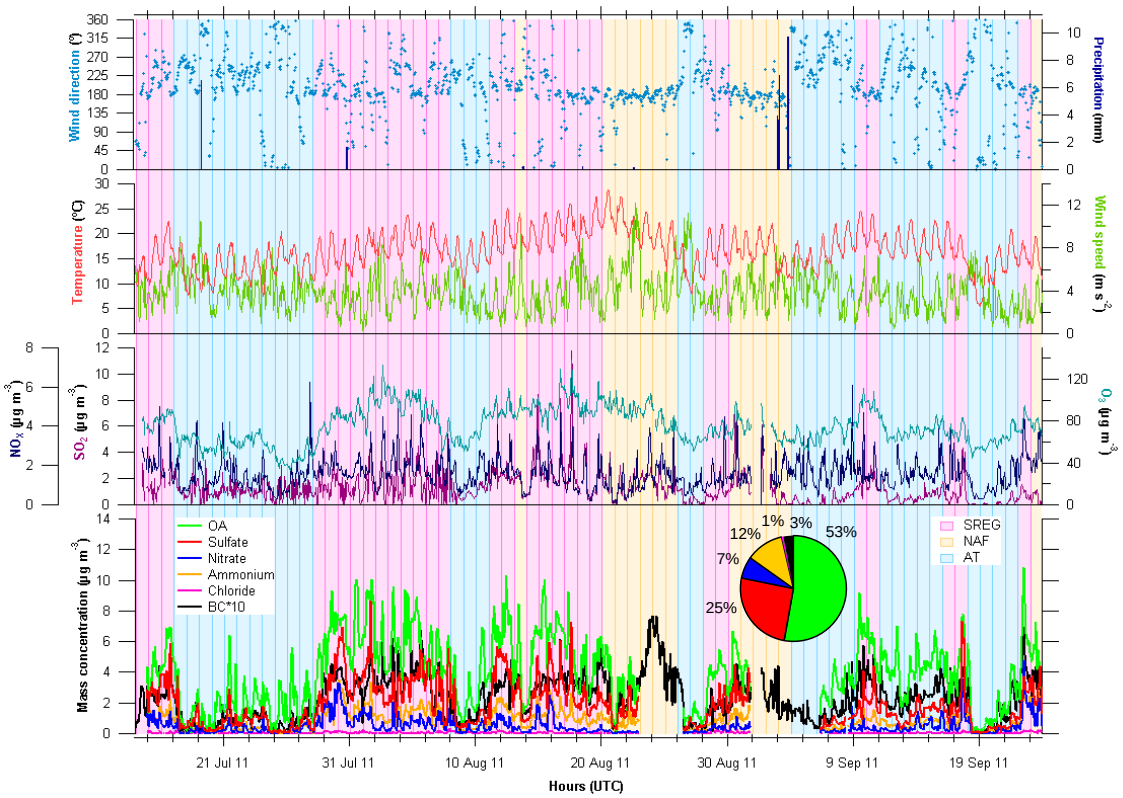

Fig. 3 Time series of wind direction, precipitation, temperature, wind speed, concentrations of nitrogen oxides (NO_x), sulfur dioxide (SO_2), ozone (O_3), and PM_1 chemical species (OA, sulfate, nitrate, ammonium, chloride and black carbon (BC)) in summer (14 Jul 11 – 24 Sep 11). Background colors correspond to daily classification of atmospheric episodes (summer regional (SREG), North African (NAF), and Atlantic (AT)) and the pie chart correspond to the average chemical composition for the summer period.

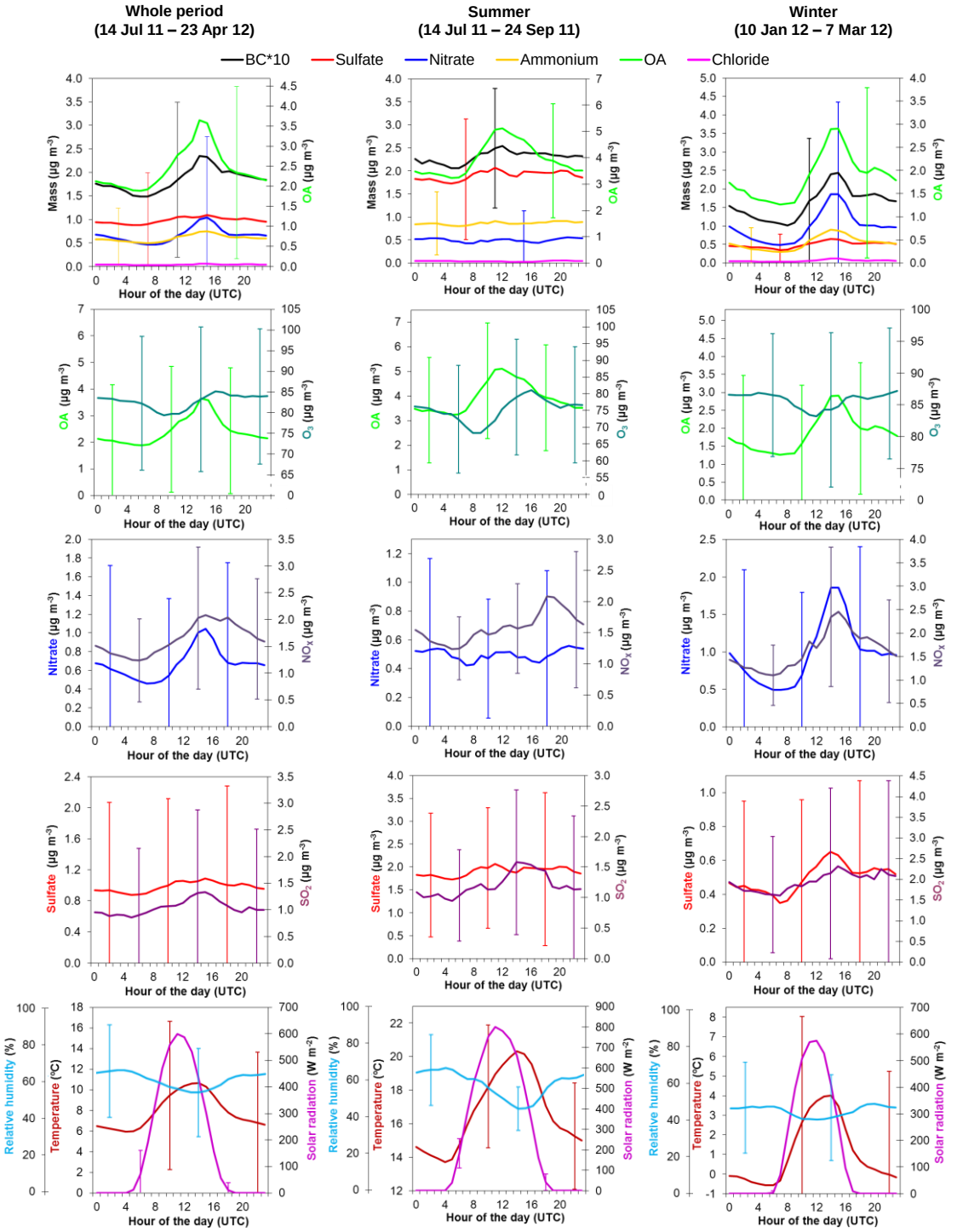

Fig. 4 Diurnal cycles of PM_1 chemical species (black carbon (BC), sulfate, nitrate, ammonium, chloride and OA), gaseous pollutants (ozone (O_3), nitrogen oxides (NO_x), and sulfur dioxide (SO_2)), and meteorological parameters (relative humidity, temperature and solar radiation) averaged for the whole period, summer and winter. Variation bars indicate ± standard deviation.

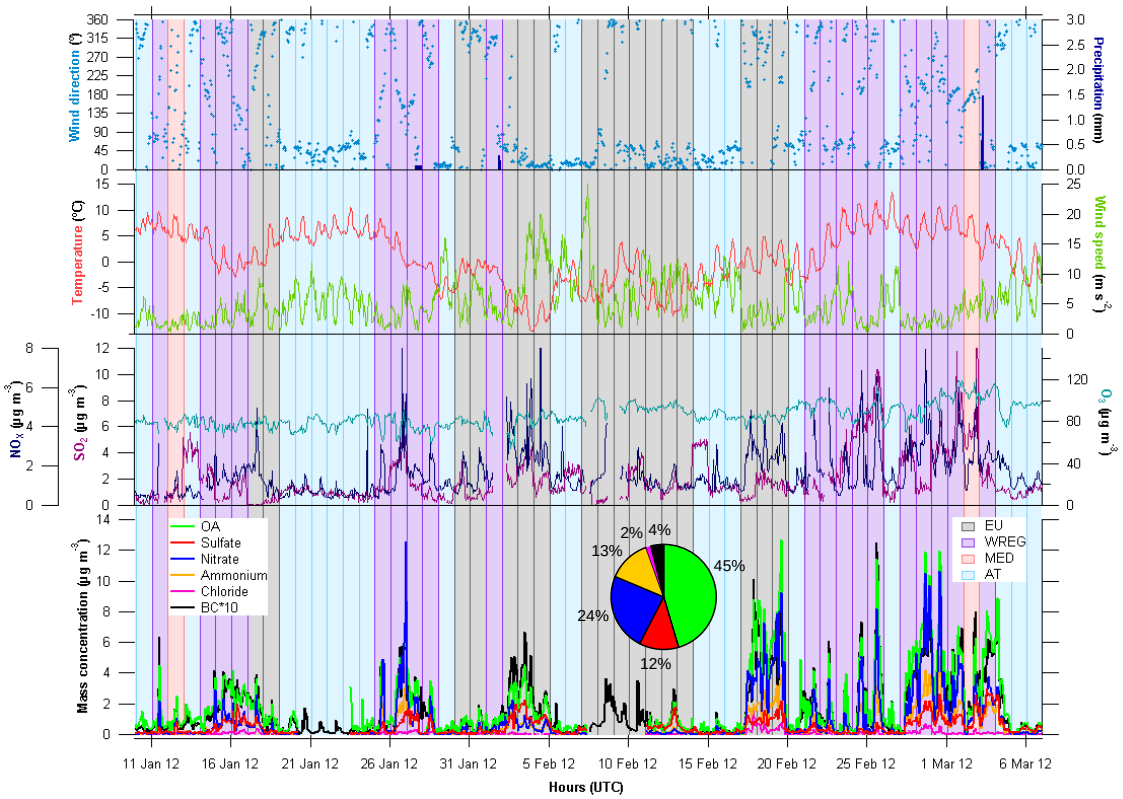

Fig. 5 Time series of wind direction (WD) and speed (WS), temperature (T), precipitation (PP), concentrations of nitrogen oxides (NO_X), sulfur dioxide (SO_2), ozone (O_3), and PM_1 chemical species (organics, sulfate, nitrate, ammonium, chloride and black carbon (BC)) in winter (10 Jan 12 – 7 Mar 12). Background colors correspond to daily classification of atmospheric episodes (European (EU), winter regional (WREG), Mediterranean (MED) and Atlantic (AT)) and the pie chart correspond to the average chemical composition for the winter period.

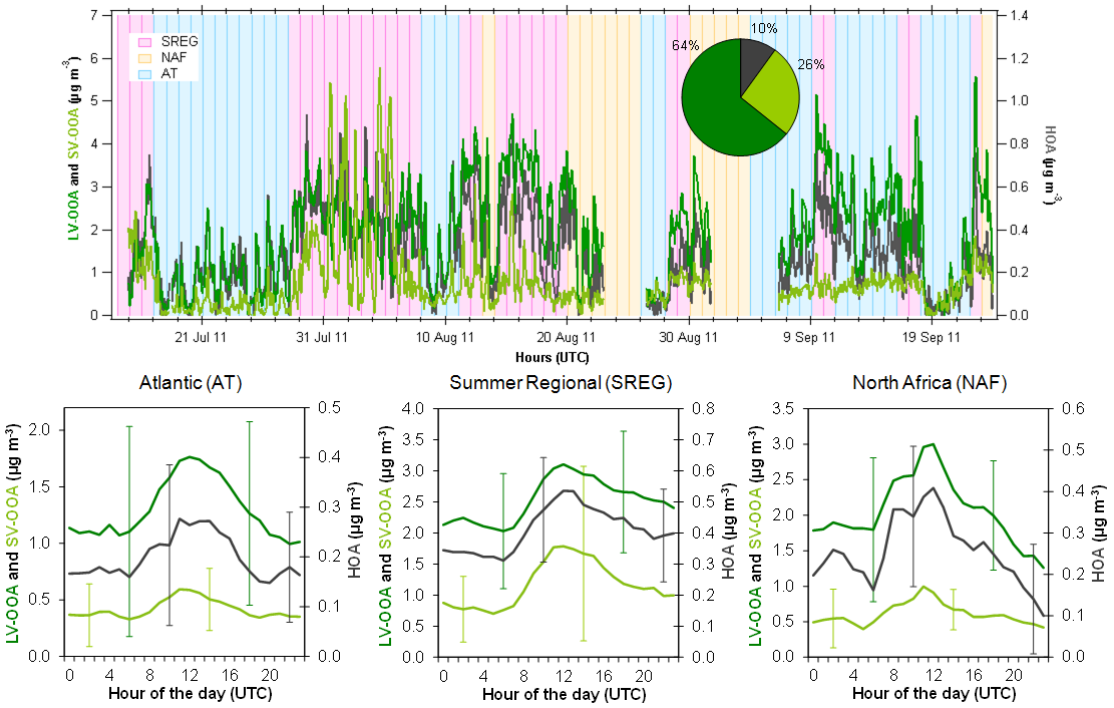

Fig. 6 Top: Time series of organic species (hydrocarbon-like organic aerosol (HOA), semi-volatile oxygenated organic aerosol (SV-OOA) and low-volatility oxygenated organic aerosol (LV-OOA)) concentrations in summer (14 Jul 11 – 24 Sep 11). Background colors correspond to daily classification of atmospheric episodes and the pie chart correspond to the average organic species composition for the summer period. Bottom: Diurnal cycles of organic species concentrations averaged as a function of atmospheric episode for the summer period. Variation bars indicate ± standard deviation.

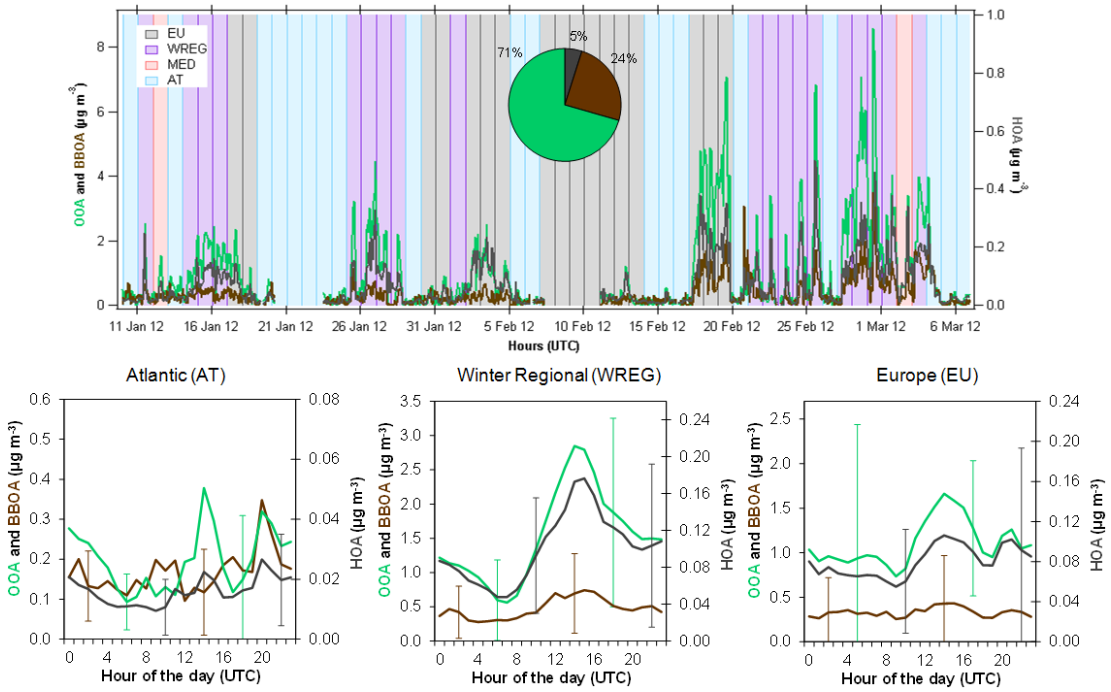

Fig. 7 Top: Time series of organic species (hydrocarbon-like organic aerosol (HOA), biomass burning organic aerosol (BBOA) and oxygenated organic aerosol (OOA)) concentrations in winter (10 Jan 12 – 7 Mar 12). Background colors correspond to daily classification of atmospheric episodes and the pie chart correspond to the average organic species composition for the winter period. Bottom: Diurnal cycles of organic species concentrations averaged as a function of atmospheric episode for the winter period. Variation bars indicate ± standard deviation.